AIChE

# Importance of Sample Intraparticle Diffusivity in Investigations of the Mass Transfer Mechanism in Liquid Chromatography

**Fabrice Gritti and Georges Guiochon**
Dept. of Chemistry, University of Tennessee Knoxville, TN 37996

*DOI 10.1002/aic.12280*
*Published online May 12, 2010 in Wiley Online Library (wileyonlinelibrary.com).*

*The effective diffusivity of a nonretained (thiourea) and of a strongly retained (phenol) compounds were measured with the peak parking method in two different columns (both 150 × 4.6 mm) packed with two types of porous particles having different mesopore sizes [5 μm Jupiter-$C_{18}$, 320 Å and Luna(2)-$C_{18}$, 100 Å]. The eluent was a methanol–water mixture (10/90 v/v) and the temperature 294 K. The effective diffusivity data acquired were used to determine the intraparticle diffusivity, $D_p$, based on two different diffusion models. The first one assumes that the diffusion fluxes across the particles and in the interparticle volume are additive (parallel diffusion model). The second model was rigorously derived on the basis of the effective medium theory of diffusion (diffusion model) in a binary composite medium (particles + interparticle volume). In both models, it was assumed that the rate of equilibrium between the liquid and the solid phases was infinitely faster than the rate of axial diffusion along the column at zero flow rate. Both models provide physically meaningful intraparticle diffusivity coefficients that take into account the average mesopore size of the particles, their specific surface area, and the retention factor of the analyte. Although the actual effective intraparticle diffusivity remains unknown, these result confirm that the mass transfer resistance due to diffusion through the porous particles has almost negligible effects in reversed phase liquid chromatography due to the importance of surface diffusion. Combining the results of the peak parking method with the h data measured at high linear velocities allows the unambiguous measurement of the film mass transfer and the surface diffusion coefficients.* © 2010 American Institute of Chemical Engineers *AIChE J*, 57: 346–358, 2011

*Keywords: mass transfer kinetics, intraparticle diffusivity, longitudinal diffusion, transparticle mass transfer resistance, external film mass transfer resistance*

## Introduction

We are not able yet to measure the parameters of all the independent kinetic terms contributing to the overall mass transfer mechanism of compounds in reversed phase liquid chromatography (RPLC). The main difficulty is that these contributions are due to different mass transfer events that cannot be isolated from each other during the series of measurements that must be made and a systematic experimental investigation is needed. For instance, correlations available in the literature are often used to express either the eddy dispersion term[1] and/or the film mass transfer coefficient[2]

Correspondence concerning this article should be addressed to G. Guiochon at guiochon@utk.edu.

between the eluent and the particles. The rest of the kinetic parameters can then be easily derived. However, these correlations were derived under experimental conditions quite different from those prevalent in RPLC and additional validation studies are required.

The mass transfer mechanism in packed bed is decomposed into three main contributions, longitudinal and eddy diffusion, and mass transfer kinetics. The first contribution or $B$-term is negligible in practice at high linear velocities. This mostly explains the relatively poor interest devoted to it in recent years[3] and why the importance of this term is underestimated, although it is directly related to the analyte diffusion across the bed of particles, diffusion that controls in part the mass transfer kinetics between the eluent and the particles.

The second contribution or $A$-term was thoroughly studied by Giddings[4] in his coupling theory of eddy dispersion in packed columns. This theory accounts well for trans-channel, short-range interchannel, and long-range interchannel velocity biases and is consistent with a reduced height equivalent to a theoretical plate (HETP) around two for well-packed columns. However, this theory could not quantitatively predict the trans-column velocity biases, which are caused by the intrinsic flow heterogeneity across the diameter of the packed bed.[5] In well-packed 4.6 mm inner diameter (I.D.) columns, the relative difference between the eluent velocities at the column center and near its wall is of the order of a few percent.[6] The corresponding reduced eddy dispersion term varies proportionally to the column length. It was recently reported that the porosity of the particles, hence the surface area available for analyte adsorption and retention, have a significant impact on the trans-column eddy dispersion term. A general expression of this term was proposed.[7]

Finally, the experimental $C$-term results essentially from the addition of the contributions of the mass transfer resistances due to analyte diffusion across the particles and to the exchange between the interstitial moving eluent and the external surface area of the porous particles.[1] The deconvolution between these two diffusion processes requires the independent measurements of the parameters of either process. In mostly all investigations of the $C$-term in packed beds, correlations are used for the determination of the film mass transfer coefficient between the moving fluid and the spherical nonporous particles.[2,8] The Wilson and Geankoplis correlation was recently validated in chromatographic columns packed with 18 $\mu$m nonporous particles.[9] It has not yet been validated with porous particles, however. The direct measurement of the film mass transfer coefficient with porous particles involves the measurement of the analyte effective particle diffusivity, $D_p$. Then, by analyzing the $h$ data over a range of high reduced linear velocities for which the eddy term remains constant (flow-controlled regime), $k_f$ can be extracted. The challenge lies in the measurement of $D_p$ in chromatographic columns because the structure of the packed bed is equivalent to that of a binary composite made of the interstitial eluent and the particles filled with the same eluent and that diffusion proceeds in both.

The principle of measuring particle diffusivity consists in measuring the effective diffusion coefficient of the analyte along the column (i.e., the $B$-term) which results from the complex combination of diffusion inside the interparticle and the particle volumes. A proper diffusion model in the binary composite medium is then necessary.

In this work, we used two models of diffusion in composite media and applied both to two different types of particles that differ in their average pore size and specific surface area and to two compounds (one nonretained and one strongly retained compound). Significant differences in the mesopore size result in measurable differences in the particle porosity, in their pore network structure, hence in different internal obstruction factors.[10] Retained compounds can diffuse onto the surface of the mesopores, hence diffuse more rapidly than unretained analytes across particles[11] if the specific surface area is large enough. A diffusion model should predict these characteristics to be acceptable and used to estimate the kinetic parameters such as the film mass transfer coefficient, $k_f$, and/or the surface diffusion coefficient, $D_S$. The first model used assumes the additivity of the mass fluxes in the interparticle and particle volumes. The second, more sophisticated model is derived from the effective medium theory of diffusion in composite media.[12] The band axial dispersion terms in the packed columns were measured using the peak parking method.[13] We discuss the physical meaning of all the values of $D_p$ found and conclude whether these diffusion models may be used to estimate the parameters of the mass transfer kinetics in packed liquid chromatography (LC) columns.

## Theory

### *Definitions*

The following definitions are necessary to present a clear theoretical development.

The volume fractions occupied by the bulk (interstitial and stagnant eluent) and the stationary (silica-based material) phases in the packed column are $\epsilon_t$ and $1 - \epsilon_t$, respectively. The volume fractions occupied by the interparticle and the particle volumes are $\epsilon_e$ and $1 - \epsilon_e$, respectively.

The local concentrations in the bulk and in the stationary phases are $c_m(t)$ and $c_s(t)$, respectively. The ratio of the stationary and bulk phase concentrations of the compound at equilibrium is the Henry's constant, $K_a$. The molecular diffusivity of the sample in the bulk eluent is $D_m$.

The sample diffusivity within the particles or the intraparticle diffusivity $D_p$ measures the effective diffusion coefficient of a compound inside individual porous particles of the packing material. The definition of this diffusion coefficient assumes that the concentration gradient in the pores is the driving force of diffusion,[14] consistent with the definition of the effective particle diffusivity in the general rate model of chromatography.[1] The value of $D_p$ results from the combination of pore and surface diffusions. The ratio of $D_p$ to the molecular diffusivity, of the compound in the bulk mobile phase is called $\Omega$.

The effective diffusion coefficient $D_{eff}(v = 0)$ of a compound through the packed bed is its apparent diffusion coefficient inside the column, at zero velocity of the mobile phase, as measured using the peak parking method. The concentration gradient in the bulk phase is the driving force of diffusion. It results from the combination of its diffusion in the interstitial column volume and the particle diffusivity. The ratio of $D_{eff}(v = 0)$ to $D_m$ of an analyte is noted $\Omega_c$.

### The classical parallel diffusion model in composite media

A detailed model for longitudinal diffusion combined with intraparticle diffusion have already been proposed by Ruthven.[15] In this work, the model assumes that the contributions of the interparticle and particle volumes to the diffusive mass flux are additive, with a weighing coefficients equal to the respective volume fractions, $\epsilon_e$ and $1 - \epsilon_e$, respectively. The diffusion coefficients in the interstitial volume and in the particle volume are $\gamma_e D_m$ and $D_p$, respectively. Note that the tortuosity and the constriction (obstruction factor $\gamma_e$) of the interstitial channels are considered in this model and that it assumes the thermodynamic equilibration between the two phases to be infinitely faster than the diffusion process, i.e., that $c_s(t) = K_a c_m(t)$ is always true everywhere in the column, at all time.

The mass balance in a column slice of width $dz$ and unit surface area $A = 1$, where the sample can only diffuse in the axial $z$-direction is

$$\epsilon_t \frac{\partial c_m}{\partial t} + (1 - \epsilon_t)\frac{\partial c_s}{\partial t} = \epsilon_e \gamma_e D_m \frac{\partial^2 c_m}{\partial z^2} + (1 - \epsilon_e) D_p \frac{\partial^2 c_m}{\partial z^2} \quad (1)$$

This equation can be simplified as

$$\frac{\partial c_m}{\partial t} = \frac{\epsilon_e \gamma_e D_m + (1 - \epsilon_e) D_p}{\epsilon_t + (1 - \epsilon_t) K_a} \frac{\partial^2 c_m}{\partial z^2} \quad (2)$$

By definition, the effective diffusion coefficient, $D_{eff}(v = 0)$, in the column is[10]

$$\frac{\partial c_m}{\partial t} = D_{eff}(v = 0) \frac{\partial^2 c_m}{\partial z^2} \quad (3)$$

$D_{eff}(v = 0)$ is a diffusion coefficient, which is directly provided by the peak parking experiments and is derived from the slope of the plot of the peak variance as a function of the parking time $t_p$ (see later in the experimental Section). By identification between Eqs. 2 and 3, the effective diffusion coefficient, $D_{eff}(v = 0)$, of a compound in the packed column, at zero flow rate and according to the pore parallel diffusion model is

$$D_{eff}(v = 0) = \frac{\epsilon_e \gamma_e D_m + (1 - \epsilon_e) D_p}{\epsilon_t + (1 - \epsilon_t) K_a} \quad (4)$$

### The effective medium theory of diffusion in composite media

The effective medium theory (EMT) of diffusion was proposed by Davis[12] as an extension of the EMT developed by Landauer[16] to describe electrical conduction in metallic inhomogeneous mixtures. The rigorous application of the EMT to the case of diffusion in a packed chromatographic bed at zero velocity is not straightforward and deserves some development that we provide in the next few sections.

### General effective conduction in composite media

Most generally, in a linear transport regime, the flux $J_i$ of either charge, mass, or heat in a homogenous medium $i$ is written as the negative of the product of the medium conductivity, $\alpha_i$, and the gradient of the corresponding driving force (voltage, chemical potential, or temperature), $F_i$

$$\vec{J}_i = -\alpha_i \vec{\nabla} F_i \quad (5)$$

Combining the continuity equation under steady-state conditions ($\vec{\nabla} \cdot \vec{J}_i = 0$ when the flux and the driving force are kept constant in the experiments) with Eq. 5 and $\alpha_i$ constant, the following condition is satisfied

$$\nabla^2 F_i = 0 \quad (6)$$

Landauer[16] treated the local inhomogeneities as fluctuations in an effective medium of conductivity $\alpha_{EMT}$ which is given by the solution of the following equation

$$\sum_i \epsilon_i \frac{\alpha_i - \alpha_{EMT}}{\alpha_i + 2\alpha_{EMT}} = 0 \quad (7)$$

where $\epsilon_i$ is the volume fraction of the homogeneous region, $i$ in the composite material. For a binary composite ($\alpha_1$ and $\alpha_2$), the effective medium conductivity is given by the positive root of the quadratic polynomial

$$\frac{\alpha_{EMT}}{\alpha_2} = a + \sqrt{a^2 + \frac{x}{2}} \quad (8)$$

with

$$x = \frac{\alpha_1}{\alpha_2} \quad (9)$$

and

$$a = \frac{1}{4}[3\epsilon_2 - 1 + x(2 - 3\epsilon_2)] \quad (10)$$

The next step of the demonstration consists in extending the effective medium theory from a charge to a mass transport regime.

### Application to the case of molecular diffusion in binary composite materials

Equation 5, written for an electric current, is simply replaced by the mass flux in each homogeneous medium, $i$, assuming again a linear transport regime

$$\vec{J}_i = -L_i \vec{\nabla} \mu_i \quad (11)$$

where $L_i$ is the Onsager coefficient (the equivalent of the coefficient $\alpha_i$ in the previous section) and $\mu_i$ is the chemical potential of the diffusing sample molecules in the medium $i$ with:

$$\vec{\nabla} \mu_i = \vec{\nabla} \mu_i^0(T) + \vec{\nabla}[RT \ln(\gamma_i c_i)] \quad (12)$$

where $\mu_i^0(T)$ is the chemical potential of the sample under standard conditions, and at temperature $T$ in the medium $i$.

We need a relationship between the Onsager coefficient and the diffusion coefficient. To simplify this problem, we consider an isothermal system and an infinitely dilute sample. Then, the standard chemical potential, $\mu_i^0(T)$, and the activity coefficient, $\gamma_i^\infty$, are constant. Accordingly, Eq. 12 becomes

$$\vec{\nabla}\mu_i = \frac{RT}{c_i}\vec{\nabla}c_i \tag{13}$$

By comparing Eq. 11 and the first Fick's law of diffusion ($\vec{J}_i = -D_i\vec{\nabla}c_i$), we obtain the fundamental link between the molecular diffusion coefficients $D_i$ (which are of interest in our work) and the phenomenological Onsager coefficient in the medium $i$

$$L_i = D_i\frac{c_i}{RT} \tag{14}$$

It is important to remember that the EMT of Landauer (Eq. 8) applies to the Onsager coefficient, $L_i$, not to the diffusion coefficients $D_i$. It follows that

$$\frac{L_{\mathrm{EMT}}}{L_2} = a + \sqrt{a^2 + \frac{1}{2}\frac{L_1}{L_2}} \tag{15}$$

The overall mass flux $J$ in the composite medium is assumed to be constant (steady-state conditions) because the gradient of chemical potential $\mu$ applied is kept constant. The effective Onsager coefficient, $L_{\mathrm{EMT}}$, is defined by

$$J = -L_{\mathrm{EMT}}\nabla\mu \tag{16}$$

In addition, we assume that the two phases are in thermodynamic equilibrium (Henry's constant $K$ at infinite dilution), so the chemical potentials are the same in both phases

$$K = \frac{c_1}{c_2} \tag{17}$$

$$\mu = \mu_1 = \mu_2 \tag{18}$$

At this stage of the development of the EMT for diffusion processes, there is no unique way to define the overall effective diffusion coefficient $D_{\mathrm{EMT}}$, which depends on which driving force is arbitrarily chosen to express the unique measurable and constant flux $J$. For reasons that will become obvious later, we define $D_{\mathrm{EMT}}$ by choosing the concentration gradient in medium 2 as the driving force

$$J = -D_{\mathrm{EMT}}\nabla c_2 \tag{19}$$

By combining Eqs. 14–19 we obtain for the local effective diffusion coefficient $D_{\mathrm{EMT}}$

$$D_{\mathrm{EMT}} = D_2\left(a + \sqrt{a^2 + \frac{1}{2}\frac{D_1}{D_2}K}\right) \tag{20}$$

where $a$ in the general Eq. 10 is equal to

$$a = \frac{1}{4}\left[3\epsilon_2 - 1 + \frac{D_1}{D_2}K(2 - 3\epsilon_2)\right] \tag{21}$$

### *Application to the determination of the effective diffusivity in packed chromatographic beds at zero flow rate*

The effective diffusion coefficient, $D_{\mathrm{EMT}}$ that is rigorously derived from the EMT is not equal to the axial diffusion coefficient, $D_{\mathrm{eff}}(v = 0)$, measured from the peak parking experiments. The mass balance equation in a slice of chromatographic column of width $dz$, where a band is allowed to diffuse axially along the column at zero flow rate, provides a relationship between these two coefficients

$$[\epsilon_t + (1 - \epsilon_t)K_a]\frac{\partial c_m}{\partial t} = D_{\mathrm{EMT}}\frac{\partial^2 c_m}{\partial z^2} \tag{22}$$

Recalling Eq. 3, we can now justify the convention chosen for the expression of $D_{\mathrm{EMT}}$, consistent with the driving force being the concentration gradient in the bulk eluent ($\bigtriangledown c_m$). Identification of the experimental problem with the EMT requires that $D_2 = D_m$, $\epsilon_2 = \epsilon_e$, and $c_m = c_2$. We also need to identify $D_1$ to the particle diffusivity $D_p$, previously defined. Also, in Eqs. 20 and 21, after the EMT theory, $D_1$ is the sample particle diffusivity with the gradient of the average particle concentration ($c_1 = Kc_2 = Kc_m$) taken as the driving force ($J_1 = -D_1\bigtriangledown c_1$). $D_1$ differs from $D_p$ which is defined by assuming that the driving force is the pore concentration gradient (or the bulk eluent concentration gradient) ($J_1 = -D_p\bigtriangledown c_2$). It is obvious to show that $D_1 = \frac{D_p}{K}$.

Finally, by combining Eqs. 22, 20, and 3, the effective diffusivity of the sample, $D_{\mathrm{eff}}(v = 0)$, predicted by the EMT theory is given by

$$D_{\mathrm{eff}}(v = 0) = \frac{D_{\mathrm{EMT}}}{\epsilon_t + (1 - \epsilon_t)K_a} = \frac{a + \sqrt{a^2 + \frac{1}{2}\frac{D_p}{D_m}}}{\epsilon_t + (1 - \epsilon_t)K_a}D_m \tag{23}$$

with

$$a = \frac{1}{4}\left[3\epsilon_e - 1 + \frac{D_p}{D_m}(2 - 3\epsilon_e)\right] \tag{24}$$

Equation 23 (EMT diffusion model) can now be directly compared to Eq. 4 (classical parallel diffusion model).

### *Moment analysis and reduced column HETP*

The first moment ($\mu_1$) and the second central moment ($\mu_2'$) of bands recorded in the parking experiment method are given by

$$\mu_1 = \frac{\int_0^\infty C(t)t\,dt}{\int_0^\infty C(t)\,dt} \tag{25}$$

$$\mu_2' = \frac{\int_0^\infty C(t)(t - \mu_1)^2\,dt}{\int_0^\infty C(t)\,dt} \tag{26}$$

## Experimental

### *Chemicals*

The mobile phases used in this work were either pure water or a water–methanol mixture (90/10 v/v). Water, methanol, dichloromethane, and *n*-nonane were all purchased from Fisher Scientific (Fair Lawn, NJ) and used without further purification. The mobile phase was filtered before use on a surfactant-free cellulose acetate filter membrane, 0.2 $\mu$m pore size (Suwannee, GA). Sodium nitrate, thiourea,

**Table 1. Physico-Chemical Properties of the Jupiter-$C_{18}$ and Luna(2)-$C_{18}$ Columns Given by the Manufacturer and Measured in our Laboratory*,†**

| Neat Silica | Jupiter | Luna(2) |
|---|---|---|
| Particle size ($\mu$m) | 4.88 | 5.09 |
| Pore diameter (Å) | 320 ± 40 | 100 ± 10 |
| Surface area ($m^2$/g) | 155 | 427 |
| Metal content (ppm) | 20.8 | 11.8 |
| Particle distribution 90%/10% | 1.95 | 1.88 |
| Bonded Phase Analysis | Jupiter-$C_{18}$ | Luna(2)-$C_{18}$ |
| Total carbon (%) | 12.96 | 17.65 |
| Surface coverage ($\mu$mol/$m^2$) | 5.48 | 3.20 |
| Endcapping | Yes | Yes |
| Packed Column Analysis | | |
| Serial number | 00F-4053-E0 | 00F-4252-E0 |
| Dimension (mm × mm) | 4.6 × 150 | 4.6 × 150 |
| Total porosity* | 0.765 | 0.640 |
| External porosity† | 0.387 | 0.361 |
| Particle porosity‡ | 0.617 | 0.437 |

*Measured by pycnometry ($CH_3OH$—$CH_2Cl_2$).
†Measured by pore-blocking experiments (*n*-nonane).
‡$\varepsilon_p = (\varepsilon_t - \varepsilon_e)/(1 - \varepsilon_e)$.

and phenol, selected as injected samples, were also from Fisher Scientific.

### *Materials*

The 150 × 4.6 mm endcapped Luna(2)-$C_{18}$ (100 Å average pore size, 427 $m^2$/g specific surface area) and Jupiter-$C_{18}$ (320 Å average pore size, 155 $m^2$/g specific surface area) columns used were gifts from the column manufacturer (Phenomenex, Torrance, CA). The total porosities of the Luna(2)-$C_{18}$ and Jupiter-$C_{18}$ column beds were measured by pycnometry[17] at 294 K, using methanol (density $\rho_{CH_3OH}$ = 0.791 ± 0.001 g/$cm^3$) and dichloromethane (density $\rho_{CH_3CN}$ = 1.326 ± 0.001 g/$cm^3$) as the two eluents. The masses of the column Luna(2)-$C_{18}$ filled with methanol or dichloromethane were 78.94565 and 79.79940 ± 0.00005 g, respectively, so $\epsilon_{t,Luna(2)\text{-}C_{18}} = 0.640 \pm 0.003$. The same masses measured with the column Jupiter-$C_{18}$ were 78.68950 and 79.70990 g, so $\epsilon_{t,Jupiter\text{-}C_{18}} = 0.765$. The complete list of physico-chemical properties of these two packing materials are given in Table 1.

### *Apparatus*

The measurements were made with a HP1090 liquid chromatograph series II (Hewlett-Packard, Palo Alto, CA). This instrument includes a ternary solvent delivery system, an auto-sampler with a 250 $\mu$L sample loop, a diode-array UV detector (cell volume 1.7 $\mu$L, sampling rate 25 Hz), a column air-oven, and a data station. From the exit of the Rheodyne injection valve to the column inlet and from the column outlet to the detector cell, the total extra-column volume of the instrument is 46 $\mu$L, measured as the apparent hold-up volume of a zero-volume union connector in place of the column. The flow-rate delivered by the three pumps was measured at column outlet, under atmospheric pressure.

The accuracy of the flow rate was checked by collecting in a 25 mL volumetric glass the mass of water during 25 min, at a flow rate set at 1 mL/min, and at 294 K. The mass of water was measured at 24.895 g. The density of pure water at 294 K is $\rho_{H_2O}$ = 0.9980 ± 0.0005 g/$cm^3$ and the expected mass (25 mL) was 24.950 g, so the flow rate accuracy delivered by the pump is −0.22%. The laboratory temperature was kept constant at 294 ± 1 K by the laboratory temperature control system.

### *Parking method experiment*

The parking method was initially designed to determine the obstruction factor $\gamma_e$ of columns packed of nonporous particles in gas chromatography[18] This method was later used to measure the obstruction coefficient of LC columns.[10,13] It is based on the determination of the band broadening caused by longitudinal diffusion along the column when no flow rate is applied. The longitudinal diffusion coefficient $D_{eff}(v = 0)$ contains the contributions of axial diffusion in the interstitial column volume and of diffusivity across the particles when the particles are porous.

Five microliters samples of dilutes solution (0.02 g/L) were injected at the desired flow rate $F_v$ or linear velocity $u_R$ (the choice of which depends on the retention factor $k'$ of the sample, $F_v$ = 0.25 mL/min with thiourea, $F_v$ = 1.00 mL/min with phenol). The linearity of the adsorption isotherm of phenol was checked by injecting 5 $\mu$L of a 0.1 and 0.5 g/L solution. Both peaks remained quasi-Guassian with no enhancement of the peak asymmetry characteristic of the absence of column overloading within the experimental concentration range. Elution is performed during the time necessary for the band to reach about half the column length. The flow is then abruptly stopped and the sample let free to diffuse along the column bed during a certain parking time $t_p$. Four different parking times (e.g., 30, 120, 300, and 480 min) were used. Finally, the mobile phase stream is resumed and the peak profiles are recorded. The longitudinal diffusion coefficient, $D_{eff}(v = 0)$, along the column is directly proportional to the slope of a plot of the measured peak variance $\mu_2'$ versus the parking time $t_p$[10]

$$D_{eff}(v = 0) = \frac{u_R^2}{2}\frac{\Delta\mu_2'}{\Delta t_p} \tag{27}$$

where $u_R$ is the linear velocity of the compound band (not the mobile phase) along the column during its migration from the inlet to the middle of the column and from the middle to the outlet of the column:

$$u_R = \frac{F_v}{\epsilon_t \pi r_c^2 (1 + k')} \tag{28}$$

where $F_v$ is the flow rate, $r_c$ the column tube radius (0.23 cm), and $k'$ the retention factor of the sample. Note that when the mesopores of the porous particles are blocked $\epsilon_t = \epsilon_e$ ($\epsilon_p = 0$) and $k' = 0$.

### *Pore-blocking experiment*

To measure the external porosity of packed or monolithic columns, it is convenient to block the mesopores of the adsorbent, preventing access of both the eluent and the probe compound. This method has the advantage of providing more precise results than the conventional inverse size-exclusion chromatographic experiments, at the cost of long

equilibration time necessary before being able to perform measurements of elution time with a relative standard deviation $<0.2\%$.[19]

Both the Luna-$C_{18}$ and Jupiter-$C_{18}$ columns were initially rinsed with 2-propanol on the HP1090 instrument for 90 min at a flow rate of 1.0 mL/min, then flushed with nonane for another 90 min by using an auxiliary pump, at a flow rate of 2.0 mL/min. The column is then replaced to the HP1090 instrument, which was first purged with 60 mL of a pure water at a flow rate of 4 mL/min in order to remove 2-propanol from the instrument. Finally, the nonane present in the interstitial void volume of the column is expelled by flushing the column with a stream of pure water, at 3.50 mL/min, until the baseline of the detector is noiseless and the first moments of successive injections of dilute $NO_3^-$ are highly reproducible. This step required 200 min or 700 mL of water, which represents nearly 700 interstitial column volumes.

## Results and Discussion

The main goal of this work is to apply first a series of experimental protocols (the details of which are given in the experimental section) that will provide accurate and precise values of $D_m$, $\epsilon_e$, $\gamma_e$, and $D_{eff}(v = 0)$. These parameters intervene in the diffusion models and must be directly measured in our experiments. Two columns packed with particles having different average mesopore sizes [Jupiter-$C_{18}$, 320 Å, and Luna(2)-$C_{18}$, 100 Å], two compounds, a retained (phenol) and a nonretained (thiourea) one, the same mobile phase (methanolwater mixture, 10/90, v/v) and laboratory temperature ($T = 294$ K) fix these experimental conditions. In a second step, the effective particle diffusivity, $D_p$, is unambiguously derived from the diffusion models, Eqs. 4 (classical parallel diffusion model) and 23 (effective medium theory model) described in the theory section. Finally, the relevance of both models to predict meaningful kinetic parameters involved in the mass transfer mechanism in RPLC is analyzed and discussed based on the characteristic of both Jupiter-$C_{18}$ and Luna(2)-$C_{18}$ porous particles and on the retention of the two analytes.

### *Determination of the external porosities, obstruction factors, and diffusion coefficients*

*Measurement of the External Porosities of the Packed Beds.* The experimental protocol used is that of pore-blocking experiments (see experimental section for details). The mesopore volume of the particles of the packed bed was filled with liquid n-nonane and the column run with pure water. One microliter of a dilute solution of sodium nitrate in water ($C < 0.02$ g/L) was injected at different flow rates and the external porosity, $\epsilon_e$, was extrapolated to a zero flow rate. The robustness of this method was demonstrated by successively increasing and decreasing the flow rate from 0 to 3.5 mL/min. The variation of the external porosity was directly related to the compressibility of *n*-nonane and the $C_{18}$-bonded chains trapped inside the mesopores.[5,7] Figures 1A,B show the plots of $\epsilon_e$ vs. the flow rate $F_v$. By extrapolation, we measured $\epsilon_e = 0.387$ and 0.361 with the Jupiter and Luna(2) columns, respectively. Note that the total pore blocking is a very precise technique to measure the external porosities of packed beds but its accuracy remains unknown because we cannot guess to which extent the crevices outside the particles are filled with *n*-nonane.

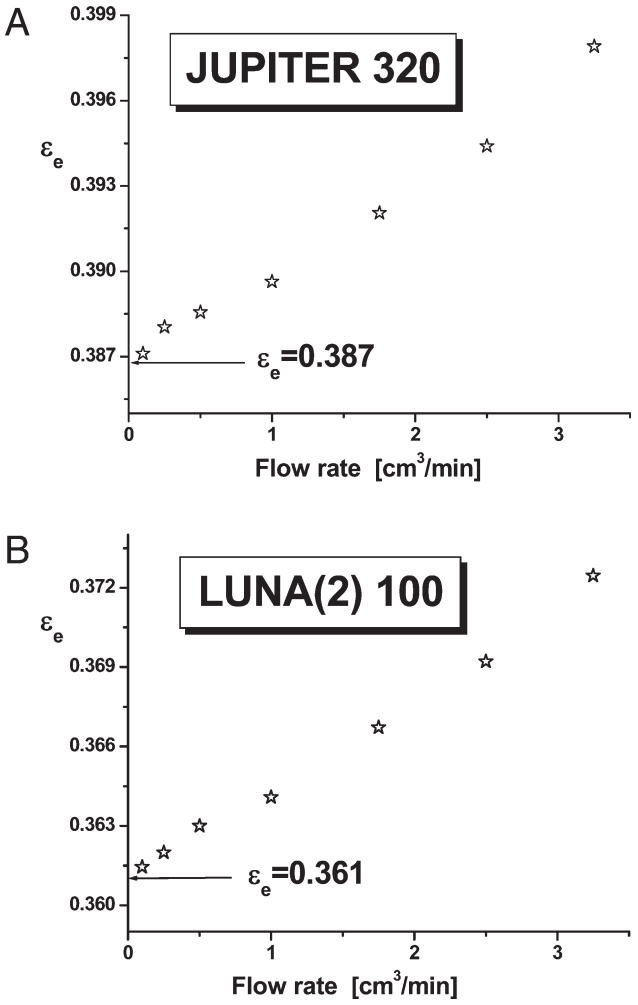


**Figure 1. Measurement of the external porosity of the Jupiter-$C_{18}$ (A) and Luna(2)-$C_{18}$ (B) columns after total blocking of the mesopores by nonane as a function of the flow rate applied.**

The decrease of the external porosity as the flow rate decreases is due to expansion of nonane and $C_{18}$-bonded chains inside the mesopores. The external porosity is measured by extrapolation of the data at a zero flow rate (see horizontal lines).

### *Measurement of the obstruction factors of the packed beds*

To measure the interstitial obstruction factors $\gamma_e$ of the packed beds, we applied the peak parking method after filling the mesopore volumes with *n*-nonane. Details about the peak parking and pore blocking experiments are given in the experimental section. Thiourea cannot penetrate the particle volumes ($D_p = 0$, $\epsilon_t = \epsilon_e$ or $\epsilon_p = 0$) as it is not retained, $K = K_a = 0$. As the mass flux is rigorously zero at the interface between the external surface of the filled particles and the moving eluent, sample diffusion must take place around

the spherical particles, in the interstitial volume (which provides the interstitial obstruction factor, $\gamma_e$). It is interesting to evaluate the results given by both models. The classical parallel diffusion model (Eq. 4) provides only a general solution for the effective sample diffusivity, $D_{eff}(v = 0)$

$$D_{eff}^{\parallel}(v = 0) = \gamma_e D_m \tag{29}$$

Experiment is definitely needed to measure $\gamma_e$. On the other hand, the EMT theory provides directly its own solution

$$D_{eff}^{EMT}(v = 0) = \frac{1}{2}\frac{3\epsilon_e - 1}{\epsilon_e} D_m \tag{30}$$

Interestingly, the EMT model offers an expression for the obstruction factor $\gamma_e$ as a function of the external porosity $\epsilon_e$. As expected, it is equal to 1 when $\epsilon_e = 1$ (no particle, hence no obstruction) and it decreases towards 0 when $\epsilon_e \rightarrow 1/3$. Below this threshold percolation porosity, $\gamma_e$ would be negative which makes no physical sense. According to the EMT theory, this means that for interstitial porosities smaller than 1/3, the eluent is no longer connected in a random composite made of a solid phase (nonporous particles, $D_p = 0$) and a liquid phase (eluent). Diffusion through the composite is then stricty zero because the eluent is simply trapped within the solid matrix. If $\epsilon_e$ is larger than 1/3, then it is possible to estimate the interstitial obstruction factor $\gamma_e$ according to the EMT model. For instance, $\gamma_e$ is equal to 0.208 and 0.115 for the Jupiter and the Luna(2) columns, respectively. It is interesting to compare these values with the experimental ones.

By positioning a zone of thiourea near to the middle of the column and letting it spread along the packed bed in pure water, at constant temperature $T = 294$ K and at a zero flow rate during various parking times $t_p$, the peak parking method allows the measurement of the effective sample diffusion, $D_{eff}(v = 0)$, along the packed column, using Eq. 27. Knowing the bulk diffusivity $D_m$, we can directly derive $\gamma_e$. The diffusion coefficient of thiourea at infinite dilution in pure water and at 298 K is experimentally known and equal to $1.33 \times 10^{-5}$ cm$^2$/s.[20,21] The viscosities of pure water at 298 K and 294 K are 0.89 cP and 0.98 cP, respectively.[1] The diffusion coefficient of thiourea in pure water and at 294 K is thus $1.21 \times 10^{-5}$ cm$^2$/s.

Figure 2 shows the results of the peak parking experiments. As expected, the peak variance ($\mu_2'$) increases linearly with the parking time, $t_p$. From the slope of these plots, the effective sample diffusivity along the column, $D_{eff}(v = 0)$, is directly measured and the value of the obstruction factor determined. We measured $\gamma_e = 0.611$ and 0.595 on the Jupiter-$C_{18}$ and Luna(2)-$C_{18}$ columns, respectively. These values are within the expected range, e.g., around 0.60, for random packing of spheres with external porosity around 0.40.[18]

In conclusion, the EMT model fails correctly to predict the experimental obstruction factors when $D_p = 0$. The bed obstruction factors predicted ($\simeq$ 0.1–0.2) are smaller than the actual ones ($\simeq$ 0.6). This result is not fundamentally surprising. By essence, the EMT theory treats local and randomly distributed inhomogeneities (the packed particles in chromatography) in the conductivity of the actual composite (the packed bed in chromatography) as fluctuations in an effective medium. This theory accounts neither for the shape nor for the contour of these inhomogeneities but only for their volume fraction. Then, it cannot provide correct physical estimates of the interstitial obstruction factor in packed beds.

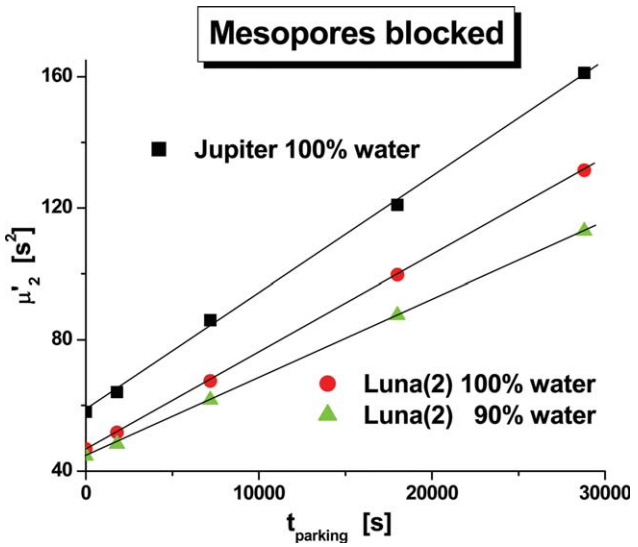


**Figure 2. Results of the peak parking experiments with the mesopores filled with *n*-nonane.**

Plots of the time variance $\mu_2'$ of thiourea vs. the parking time $t_p$ in the Jupiter (full squares) and Luna(2) (full circles and triangles) columns. The flow rate used to place the sample zone at half the length of the column was 0.25 mL/min. $T = 294$ K. Two different eluent compositions (pure water and methanol–water mixture, 10/90, v/v) were applied to study the effective diffusion of thiourea in the Luna(2) column. [Color figure can be viewed in the online issue, which is available at wileyonlinelibrary.com.]

### *Measurement of the molecular diffusion coefficient of thiourea and phenol in a mixture of water and methanol*

Knowing the diffusion coefficients of thiourea and phenol in the methanol-water mixture (10/90, v/v) at $T = 294$ K is also needed . The diffusion coefficient of thiourea was measured by repeating the peak parking experiments with the Luna(2)-$C_{18}$ column and by replacing the eluent pure water with this methanol–water mixture. The results are given in Figure 2 (full green triangles). We observed that the slope of the plot decreases when 10% methanol was added into pure water, which is consistent with the increase of the eluent viscosity, explaining the decrease of the sample diffusion coefficient. We measured $D_{eff}(v) = 5.74 \times 10^{-6}$ cm$^2$/s. As the obstruction factor is a structural parameter, it should be independent of the nature of the eluent. So, $\gamma_e = 0.595$ and the diffusion coefficient of thiourea, at 294 K and in the methanol–water mixture containing 10% methanol in volume, is equal to $9.65 \times 10^{-6}$ cm$^2$/s. This method provides the diffusion coefficient of thiourea with great accuracy and precision, provided a reference value of $D_m$ is known under well-defined standard conditions.

Unlike with thiourea, we could not repeat the peak parking measurements with phenol because this compound would be absorbed by *n*-nonane inside the mesopores of the particles. Phenol would have access to the mesopore volume and would be strongly retained and concentrated in the

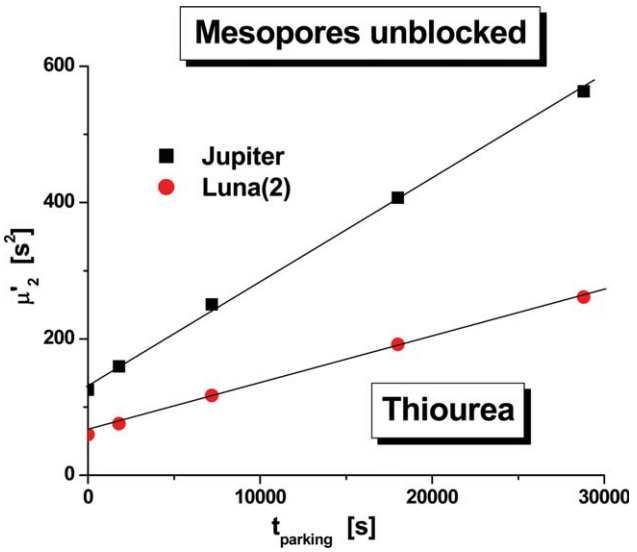


**Figure 3. Same as in Figure 2, except the mesopores were accessible to the nonretained compound thiourea.**

Mobile phase: methanol–water mixture, 90/10, v/v. Note the larger slope measured with the Jupiter-$C_{18}$ particles. [Color figure can be viewed in the online issue, which is available at wileyonlinelibrary.com.]

mesopore volume. The partition coefficient of phenol between liquid *n*-octadecyl and liquid water is quite large ($\log P_{C18/H_2O} = 1.9$)[22] Its diffusion coefficient could thus not be directly measured by pore blocking experiments. It can be derived from the known molar volume of thiourea and phenol, estimated from the LeBas group method correlation[23] (77.0 and 103.4 $cm^3$/mol). We assumed that the diffusion coefficients[24] are inversely proportional to $V_b^{0.6}$. Accordingly, the diffusion coefficient of phenol is estimated at $8.08 \times 10^{-6}$ $cm^2$/s in the methanol–water mixture and at 294 K.

### *Determination of the effective particle diffusivity of thiourea and phenol*

To acquire the data used in this section, the eluent was a 10/90 (v/v) methanol–water mixture and n-nonane was removed from the mesopores by washing the column with 2-propanol. The analyte molecules have now access to the internal volume of the particles and $D_p \neq 0$. Molecules can be adsorbed onto the walls of the mesopores and can diffuse through the particles through a combination of pore and surface diffusion. We considered two compounds, a nonretained one (thiourea) and a strongly retained one (phenol). The reason for this choice was the large difference expected between their particle diffusivities, providing a test of the ability of the diffusion models to predict correct values of these diffusivities. Surface diffusion usually accounts for more than 80% of the total particle diffusivity with retained samples.[11]

### *Nonretained samples: thiourea*

The diffusion coefficient of thiourea is $D_m = 9.65 \times 10^{-6}$ $cm^2$/s. Because thiourea is not adsorbed onto the solid phase, surface diffusion is zero and $K_a = 0$ (or $K = \epsilon_p$). The general expression of the particle diffusivity, $D_p$ is:

$$D_p = \epsilon_p \gamma_p D_m \tag{31}$$

where $\epsilon_p$ is the particle porosity, 0.617 and 0.417 for Jupiter-$C_{18}$ and Luna(2)-$C_{18}$ particles, respectively. $\epsilon_p$ accounts for the fact that the volume fraction complementary of the particle ($1 - \epsilon_p$) does not participate to particle diffusivity. $\gamma_p$ ($< 1$) is the obstruction factor, due to the tortuosity, the constriction, and the hindrance diffusion factor of the internal channels. Its value is unknown.

The theoretical expression of $D_{eff}(v = 0)$, according to the classical parallel diffusion model, is now

$$D_{eff}^{\parallel}(v = 0) = \frac{\epsilon_e \gamma_e + (1 - \epsilon_e)\epsilon_p \gamma_p}{\epsilon_t} D_m \tag{32}$$

The theoretical expression of $D_{eff}(v = 0)$ according to the EMT diffusion model is:

$$D_{eff}^{EMT}(v = 0) = \frac{a + \sqrt{a^2 + \frac{1}{2}\epsilon_p \gamma_p}}{\epsilon_t} D_m \tag{33}$$

with

$$a = \frac{1}{4}\left[3\epsilon_e - 1 + \epsilon_p \gamma_p (2 - 3\epsilon_e)\right] \tag{34}$$

In both Eqs. 32 and 33, $\gamma_p$ is the only unknown parameter. It can be directly estimated from the measurement of $D_{eff}(v = 0)$ by the peak parking method. The results of the peak parking experiments are given in Figure 3. They clearly show that the band broadening of thiourea increases faster with increasing parking time in the Jupiter than in the Luna(2) columns. On these columns, we measured $D_{eff} = 7.22 \times 10^{-6}$ and $4.62 \times 10^{-6}$ $cm^2$/s, respectively. The unique solution $\gamma_p$ that matches experimental and theoretical $D_{eff}(v = 0)$ values are listed in Table 2. These values make sense as the internal obstruction factor of Jupiter-$C_{18}$ particles is larger than that of the Luna(2)-$C_{18}$ particles. This was a priori expected because the average mesopore size of the Jupiter-$C_{18}$ particles is three times larger than that of the Luna(2)-$C_{18}$ particles (320 Å vs. 100 Å).

Both models agree qualitatively well, providing meaningful internal obstruction factors according to the data measured with a non-retained sample. In the next section, we consider a strongly retained sample, phenol, for which particle diffusivity is faster due to surface diffusion.

### *Strongly retained sample: phenol*

The diffusion coefficient of phenol is $D_m = 8.08 \times 10^{-6}$ $cm^2$/s. Phenol is strongly adsorbed on both columns, with

**Table 2. Particle Obstruction Factor**

| | Particle Obstruction Factor ($\gamma_p$) | |
|---|---|---|
| | Parallel Model | EMT Model |
| Jupiter-$C_{18}$ | 0.889 | 0.617 |
| Luna(2)-$C_{18}$ | 0.329 | 0.291 |

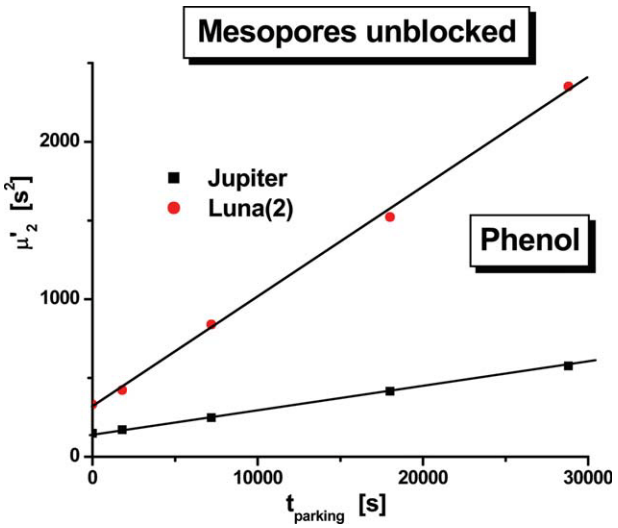


**Figure 4. Same as in Figure 3, except the strongly retained sample, phenol.**

Note that the slope of the plot measured with the Luna(2) column is now larger than that measured in the Jupiter-$C_{18}$ column. [Color figure can be viewed in the online issue, which is available at wileyonlinelibrary.com.]

$K_a = 20.8$ and 27.4 on Jupiter and Luna(2) columns, respectively. Phenol can diffuse through the particles by either the pore or the surface diffusion processes. The value of the effective sample diffusivity, $D_p$, is unknown. It will be estimated using Eqs. 4 and 23, given the experimental values of $D_{eff}(v = 0)$ determined from the peak parking experiments.

Figure 4 shows the plot of the peak variance of phenol vs. the parking time for both columns. The width of the zone of phenol increases faster with increasing parking time in the Luna(2) than in the Jupiter column. The opposite is true for the nonretained compound (see Figure 3). The reason is due to the different specific surface areas of the two adsorbents. The surface areas of the neat silicas were previously estimated at 121 and 414 $m^2$ for the Jupiter and Luna(2) columns, respectively.[7] Surface diffusion is proportional to the surface area,[14] thus is more important in the Luna(2) than in the Jupiter column. Clearly, surface diffusion dominates particle diffusivity in RPLC for retained compounds. The $D_p$ values are given in Table 3. Both models give calculated values that agree reasonably well with the effective column diffusivity, knowing $D_m$ and $D_p$. $D_p$ is undoubtedly larger in the Luna(2)-$C_{18}$ than in the Jupiter-$C_{18}$ particles, by a factor that is very close to the ratio of the surface areas of these two adsorbents.

**Table 3. Effective Intraparticle Diffusivity $D_p$ of Phenol at 295 K**

| | Effective Intraparticle Diffusivity, $D_p$ ($cm^2/s$) | |
|---|---|---|
| | Parallel Model | EMT model |
| Jupiter-$C_{18}$ | 1.87E-05 | 1.76E-05 |
| Luna(2)-$C_{18}$ | 4.95E-05 | 5.70E-05 |

### *Comparison between the parallel and the EMT diffusion model*

In the previous sections, it was shown that both diffusion models provide meaningful estimates of the kinetic parameters, for nonretained (internal obstruction factor $\gamma_p$) as well as for strongly retained (effective particle diffusivity $D_p$) compounds. The EMT model fails only when $\Omega = 0$ ($D_p = 0$ or mesopores blocked). Then, it provides an undestimated value of the obstruction factor of the interstitial channels.

It is interesting to plot the longitudinal diffusion coefficient in the column at zero flow rate $((\epsilon_t + (1 - \epsilon_t) K_a) D_{eff}(v = 0)/D_m = (\epsilon_t + (1 - \epsilon_t) K_a) \Omega_c)$ as a function of the particle diffusivity ($\Omega = D_p/D_m$) to assess the differences between the predictions of the parallel and the EMT diffusion models. Typically, $\Omega$ increases from zero (no diffusion through the particles or mesopore blocked), or 0.25 to 0.50 (for $k' \simeq 0$ with accessible mesopores) to values close to seven (for $k'$ of the order of 20). Figure 5 shows this function with $\epsilon_e = 0.40$ and $\gamma_e = 0.60$, values that are typical of commercial packed columns. For all values of $k' > 0$ and $\Omega_c$, the particle diffusivity, $D_p = \Omega D_m$, predicted by the parallel and the EMT diffusion models never differ by more than 25%. This suggests that both models are acceptable to describe the apparent sample diffusion in packed chromatographic beds.

Still, the values of $D_p$ derived according to these two diffusion models are not necessarily the correct ones. At least one of these models needs to be validated by some independent measurement of $D_p$. Another solution to the problem would consist in simulating the diffusion problem in a binary composite represented by a random distribution of spheres (particles) in a matrix medium (interparticle eluent).

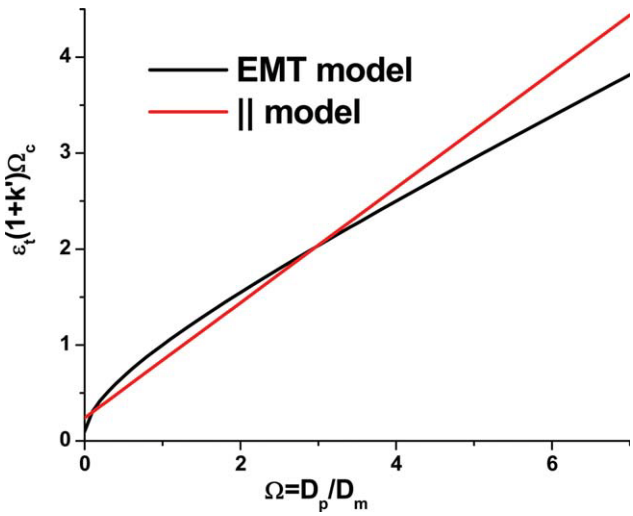


**Figure 5. Plot of the ratio of the effective axial column diffusivity, $\epsilon_t$ (1 + $k'$) $D_{eff}(v = 0)$ and the bulk diffusion coefficient, $D_m$, as a function of the ratio of the particle diffusivity, $D_p$, and $D_m$ ($\Omega$), according to the parallel and EMT diffusion models.**

Note the weak deviation between the two models. [Color figure can be viewed in the online issue, which is available at wileyonlinelibrary.com.]

### *Importance of the determination of the true mass transfer mechanism in RPLC*

We have shown that both the parallel and the EMT diffusion models allow the determination of meaningful effective particle diffusivity coefficients, $D_p$. The knowledge of this kinetic parameter is of paramount importance in the investigation of mass transfer mechanisms in RPLC.

Assuming true the value provided by either one of the diffusion models, it would be possible to determine accurately the values of important kinetic parameters in liquid chromatography, such as the film mass transfer coefficient between the eluent percolating through the column bed and the external surface area of the particles, $k_f$, and the surface diffusion coefficient, $D_S$. In the next two sections, we describe several strategies available to derive these two parameters.

### *Measurement of the film mass transfer coefficient* $\mathbf{k}_f$

The film mass transfer coefficient $k_f$ was experimentally shown to depend on whether the particles were porous[5] or nonporous[2,8,9] It is maximum with nonporous particles because the local concentration gradients at the periphery of the particle are larger than those with porous particles. Accordingly, $k_f$ should be best measured with the very same packing material studied rather than with ideal nonporous systems. First, the contribution of the trans-particle mass transfer resistance to the overall C-term is determined from the previous models Eqs. 4 and 23. Then, one measures the experimental $h$ data at high flow rates where the eddy dispersion term (A term) is about constant (flow dispersion regime). By simple difference as shown below, the coefficient $k_f$ can be estimated.

The effective particle diffusivity, $D_p = \Omega D_m$, determines the contribution of the mass transfer resistance due to analyte diffusion across the particles. The corresponding reduced HETP term, $C_p v$, was derived for spherical particles[1,25]

$$C_p v = \frac{1}{30}\frac{\epsilon_e}{1-\epsilon_e}\left(\frac{\delta_0}{1+\delta_0}\right)^2 \frac{1}{\Omega} v \tag{35}$$

where

$$\delta_0 = \frac{1-\epsilon_e}{\epsilon_e}\left[\epsilon_p + (1-\epsilon_p)K_a\right] \tag{36}$$

Equation 35 provides a direct measurement of the mass transfer coefficient $C_p$. It becomes possible to estimate the film mass transfer resistance term $C_f v$ at high reduced linear velocity $v$ where the overall eddy dispersion $A$-term becomes constant ($h \simeq A/d_p + C_p v + C_f v$). According to[1] the film mass transfer resistance reduced HETP term for spherical particles writes

$$C_f v = \frac{1}{3}\frac{\epsilon_e}{1-\epsilon_e}\left(\frac{\delta_0}{1+\delta_0}\right)^2 \frac{D_m}{k_f d_p} v \tag{37}$$

The general expression of $k_f$ for spherical particles is given by the Sherwood number[2,8] $\mathrm{Sh} = \frac{k_f d_p}{D_m} = \alpha v^{1/3}$. The power 1/3 is related to the geometry of the solid adsorbent. The experimental value of $\alpha$ should be compared to those empirically derived from the Wilson and Geankoplis ($\alpha = \frac{1.09}{\epsilon_e^{2/3}}$) and Kataoka [$\alpha = 1.85\ (1-\epsilon_e)^{1/3}$] correlations. Recent investigations and application of the parallel model of diffusion in packed[5,7] and in monolithic[26] columns have shown that the actual $\alpha$ values are at least half smaller than those provided by these correlations. The same approach was recently applied to the measurement of the external film mass transfer resistance of large, partially excluded biomolecules.[27] These investigations demonstrate that, whatever the size, small or large, of the molecules analyzed, the contribution of the external film mass transfer resistance to band broadening is the most important of all the contributions responsible for the magnitude of the $C$ term in the plate height equation.

### *Surface diffusion coefficient* $\mathbf{D}_S$

Surface diffusion gives the largest contribution to the particle diffusivity of retained samples. In the case of phenol, $D_p$ is about five times larger than the bulk molecular diffusion coefficient, $D_m$, providing a significant gain in column efficiency. This is the main explanation of the unquestionable success of RPLC. In the absence of surface diffusion, the $C_p$ coefficient would be up to five times larger than what is actually measured.

There are two possible ways to model the role of surface diffusion in particle diffusivity. First, if the surface diffusion coefficient is related to the surface area accessible in the particle (which is actually the case), and if a parallel pore/surface diffusion process is assumed (addition of both diffusion fluxes), the general expression of the particle diffusivity is[14]

$$D_p = \epsilon_p \gamma_p D_m + 2\epsilon_p \gamma_p \frac{\alpha_p}{r_p} K_a D_S \tag{38}$$

In Eq. 38, $r_p$ is the volume average pore size radius and $\alpha_p$ is a structural parameter of the silica-bonded porous particles, given by

$$\alpha_p = \frac{1}{\rho_{BP}\ \%\ \text{Silica}\ S_p} \tag{39}$$

where $\rho_{BP}$ is the density of the packing material (e.g. the sum of the masses of silica and $C_{18}$-bonded chains divided by the sum of their volume), %Silica, the silica content in the or the mass percent of neat silica in the packing material, and $S_p$, the specific surface area of the neat silica.

The determination of $D_S$ becomes straightforward according to Eq. 38, knowing the experimental value of $D_p$. This surface diffusion coefficient is physically meaningful because it refers to the actual surface area accessible inside the particles.

A second apparent surface diffusion coefficient can be derived from the EMT diffusion model assuming that the analyte could hypothetically diffuse across the solid particle's volume. In fact, it cannot as silica is impermeable but this definition is often used in the literature.[11] The calculation of the effective particle diffusivity is strictly similar to that of $D_{eff}(v=0)$ developed in the theory section. The diffusion coefficients $D_1$ and $D_2$, the volume fraction $\epsilon_2$ and the equilibrium constant $K = c_1/c_2$ in Eqs. 20 and 21 must be identified to apply this diffusion problem to this new system.

The solid particle volume is medium 1 ($J_1 = -D_1 \nabla c_1 = -D_S \nabla c_s$) and the mesopore volume is medium 2 ($J_2 = -D_2 \nabla c_2 = -F(\lambda_m) D_m \nabla c_m$, $\epsilon_2 = \epsilon_p$). $F(\lambda_m)$ is the hindrance pore diffusion factor that takes into account the ratio $\lambda_m$ of the sample size to the mesopore diameter. $K = c_s/c_m = K_a$. Consistent with the definition of $D_p$, we chose the concentration gradient in medium 2 (stagnant eluent in the mesopores) as the driving force to express the effective particle diffusivity, $D_{EMT}$, ($J = -D_{EMT} \nabla c_2 = -D_p \nabla c_m$). Hence,

$$D_p = F(\lambda_m) D_m \left( a + \sqrt{a^2 + \frac{1}{2} \frac{D_S}{D_m} \frac{K_a}{F(\lambda_m)}} \right) \tag{40}$$

where $a$ in the general Eq. 40 is equal to:

$$a = \frac{1}{4} \left[ 3\epsilon_p - 1 + \frac{D_S}{D_m} \frac{K_a}{F(\lambda_m)} (2 - 3\epsilon_p) \right] \tag{41}$$

Equations 40 and 41 allow the determination of the unique value of $D_S$ provided by the experimental data for $D_p$.

## Conclusions

The results of our investigations reported in this article demonstrate that the contribution of the external film mass transfer resistance to band broadening is the most important of all these contributions at high flow velocities. This conclusion is valid for all molecules, small (as shown in this work) or large (as shown for proteins in a more recent publication[27]). The contribution of intraparticle diffusion, although small, is not entirely negligible and it can be measured with a reasonable precision (ca. 5%). It should be determined if accurate determinations of the contribution of the external film mass transfer resistance to band broadening is needed.

Two classical diffusion models provide calculated values of the effective longitudinal diffusion coefficients of small molecules in packed columns at zero flow rate. Chromatographic beds are made of randomly distributed bulk eluent (interparticle volume) and porous adsorbent particles. The diffusion coefficients of analytes are different in these two media. The first model is based on the addition of the diffusion fluxes in the interstitial eluent and the particles. The second model is derived from the general effective medium theory of molecular diffusion. The ability of these models to predict meaningful particle diffusivities was tested for two packing materials, the particles of which contain mesopores of widely different sizes [Luna(2), 100 Å and Jupiter, 320 Å]. A nonretained (thiourea) and a strongly retained (phenol) analytes were chosen. The error of measurement of the peak parking method is smaller than 5%. The accuracy of the particle diffusivity obtained depends on the ability of the diffusion models correctly to predict the longitudinal diffusion coefficient. Both models provide physically acceptable values of the internal obstruction factors ($\gamma_p$) and the particle diffusivity coefficients ($D_p$), consistent with the differences in porosities, average mesopore sizes of the particles, and surface diffusion coefficients in RPLC mode. Still, it is impossible to tell whether these models provide the true values of $D_p$. This would require correct estimates of the contributions to mass transfer resistances due to diffusion through the porous particles. Independent and additional measurements of $D_p$ are still necessary in order to definitely validate or reject either of these two diffusion models. At this stage of our investigation, we conclude that neither diffusion model can be rejected. Both should be used in further analyses of the particle diffusivities of all analytes, nonretained, weakly, or strongly retained.

The external film mass transfer resistance contribution to the HETP of chromatographic columns can be derived from the results of measurements of reduced HETP data at high velocities and of experimental determinations of the mass transfer resistance due to trans-particle diffusion. In previous reports, this last contribution to the general HETP equation is generally assumed to be given by one of the correlations available in the literature (Wilson and Geankoplis, Kataoka). We showed that a combination of the results of the peak parking method and of either one of the two models that we developed allows the easy determination of the trans-particle diffusivities of partially excluded molecules, such as those of proteins. Due to the rapid development of the analytical and preparative applications of HPLC to the separation of proteins, the determination of such diffusion coefficients is becoming of paramount importance because protein diffusion is strongly hindered within porous silica media. The recent progress made in the preparation of shell particles[28–30] illustrate the importance of controlling protein diffusion through particles of packing media. The models developed in this work will permit the optimization of the design of these particles and that of the experimental conditions of their use. They will also allow the successful direct determination of other kinetic parameters important in RPLC, such as the film mass transfer coefficient, $k_f$, and the surface diffusion coefficients, $D_S$. Measuring indirectly $D_p$ from the results of peak parking experiments eliminates the need to recourse to empirical correlations that have not yet been fully validated for columns packed with porous particles. The precision of the results is directly related to the precision of the peak parking experiments. Finally, we note that, provided that the nature of the silica-bonded material, its porosity, its pore size distribution, its tortuosity, constriction and connectivity remain the same, the particle diffusivity is independent of the particle diameter.

## Acknowledgments

This work was supported in part by grant CHE-06-08659 of the National Science Foundation and by the cooperative agreement between the University of Tennessee and the Oak Ridge National Laboratory. We thank Tivadar Farkas (Phenomenex, CA) for the generous gift of the Jupiter and Luna(2) columns.

## Notation

### *Roman letters*

$a$ = coefficient in Eq. 8
$A$ = eddy dispersion coefficient (m)
$c_i$ = sample concentration in homogeneous medium $i$ (kg/m$^3$)
$c_m(t)$ = sample mobile phase concentration at time $t$ (kg/m$^3$)
$c_s(t)$ = sample stationary phase concentration at time $t$ (kg/m$^3$)

$C_f$ = film solid–liquid mass transfer coefficient
$C_p$ = transparticle solid–liquid mass transfer coefficient
$D_i$ = sample diffusion coefficient in homogeneous medium $i$ ($m^2/s$)
$D_{eff}(v=0)$ = apparent axial diffusion coefficient of the column at zero flow rate ($m^2/s$)
$D_{eff}^{\parallel}(v=0)$ = apparent axial diffusion coefficient of the column at zero flow rate predicted by the parallel diffusion model ($m^2/s$)
$D_{eff}^{EMT}(v=0)$ = apparent axial diffusion coefficient of the column at zero flow rate predicted by the effective medium theory diffusion model ($m^2/s$)
$d_p$ = average particle size (m)
$D_p$ = effective particle diffusivity with the mesopores' concentration gradient as the driving force ($m^2/s$)
$D_m$ = bulk molecular diffusion coefficient ($m^2/s$)
$D_{EMT}$ = effective diffusivity in the composite media with the concentration gradient in the homogeneous medium 2 as the driving force ($m^2/s$)
$F(\lambda_m)$ = pore steric hindrance parameter
$F_i$ = driving force in medium $i$ (variable unit)
$F_v$ = flow rate ($m^3/s$)
$h$ = total reduced column HETP
$J_i$ = flux in medium $i$ ($mol/m^2/s$)
$k'$ = retention factor
$K$ = equilibrium ratio of the concentrations in the homogeneous media 1 to 2
$K_a$ = equilibrium ratio of the concentrations in the stationary and bulk phases (Henry's constant)
$k_f$ = film mass transfer coefficient (m/s)
$L_{EMT}$ = effective Onsager coefficient in the binary composite material ($mol\ s/m^3$)
$L_i$ = Onsager coefficient in medium $i$ ($mol\ s/m^3$)
$r_c$ = internal column tube radius (m)
$r_p$ = average pore radius in volume (m)
$R$ = ideal gas constant (J/mol/K)
%Silica = mass content of neat silica in the bonded material
$S_p$ = specific surface area of the neat silica ($m^2/g$)
$t_p$ = parking time (s)
$t$ = time variable (s)
$T$ = temperature (K)
$u_R$ = sample migration linear velocity (m/s)
$V_b$ = molar volume of the sample at its boiling point ($m^3/mol$)
$x$ = ratio of the conductivities $\alpha_1$ and $\alpha_2$.
$z$ = axial coordinate along the column

### *Greek letters*

$\alpha$ = constant parameter in the expression of the film mass transfer coefficient $k_f$
$\alpha_{EMT}$ = effective conductivity of the composite medium
$\alpha_i$ = conductivity of homogeneous medium $i$
$\alpha_p$ = structural parameter defined in Eq. 39
$\delta_0$ = retention parameter defined in Eq. 36
$\epsilon_e$ = external column porosity
$\epsilon_i$ = fraction volume of homogeneous medium $i$
$\epsilon_p$ = particle porosity
$\epsilon_t$ = total column porosity
$\gamma_e$ = external obstructive factor of the packed bed
$\gamma_i$ = activity coefficient of the sample in homogeneous medium $i$
$\gamma_p$ = internal obstructive factor of the porous particles
$v$ = reduced interstitial linear velocity
$\Omega$ = ratio of the effective particle diffusivity to the bulk diffusion coefficient
$\Omega_c$ = ratio of the apparent axial diffusion coefficient of the column at zero flow rate to the bulk diffusion coefficient
$\mu_1$ = first moment (s)
$\mu_2'$ = second central moment ($s^2$)
$\mu_i$ = chemical potential of the sample in the homogeneous medium $i$ (J/mol)
$\mu_i^0(T)$ = chemical potential of the sample in the homogeneous medium $i$ in standard conditions and at temperature $T$ (J/mol)
$\rho_{BP}$ = density of the bonded phase material ($kg/m^3$)

## Literature Cited


1. Guiochon G, Felinger A, Katti A, Shirazi D. *Fundamentals of Preparative and Nonlinear Chromatography*, 2nd ed. Boston, MA: Academic Press, 2006.
2. Wilson E, Geankoplis C. Liquid mass transfer at very low Reynolds number in packed beds. *J Ind Eng Chem (Fundam)*. 1966;5:9–14.
3. Broeckhoven K, Cabooter D, Lynen F, Sandra P, Desmet G. Errors involved in the existing B-term expressions for the longitudinal diffusion in fully porous chromatographic media. Part II: Experimental data in packed columns and surface diffusion measurements. *Chem Eng Sci*. 2006;61:7636–7650.
4. Giddings J. *Dynamics of Chromatography*. New York, NY: Marcel Dekker, 1965.
5. Gritti F, Guiochon G. New insights on mass transfer kinetics in chromatography. *AIChE J*. 2011;57:333–345.
6. Abia J, Mriziq K, Guiochon G. *J Chromatogr A*. 2009;1216:3185–3191.
7. Gritti F, Guiochon G. Impact of retention on transcolumn eddies in packed columns. *J Chromatogr A*. In press.
8. Kataoka T, Yoshida H, Ueyama K. Mass transfer in laminar region between liquid and packing material surface in the packed bed. *J Chem Eng Jpn*. 1972;5:132–136.
9. Miyabe K, Ando M, Ando G N Guiochon. External mass transfer in high performance liquid chromatography systems. *J Chromatogr A*. 2008;1210:60–67.
10. Gritti F, Guiochon G. Effect of the surface coverage of $C_{18}$-bonded silica particles on the obstructive factor and intraparticle diffusion mechanism. *Chem Eng Sci*. 2006;61:7636–7650.
11. Miyabe K, Takeuchi S. Surface diffusion of alkylbenzenes on octadecylsilyl-silica gel. *Ind Eng Chem Res*. 1998;37:1154–1158.
12. Davis H. The effective medium theory of diffusion in composite media. *J Am Ceram Soc*. 1977;60:499–501.
13. Miyabe K, Matsumoto Y, Guiochon G. Peak parking-moment analysis. A strategy for the study of the mass-transfer kinetics in the stationary phase. *Anal Chem*. 2007;79:1970–1982.
14. Gritti F, Guiochon G. General HETP equation for the study of mass transfer mechanisms in RPLC. *Anal Chem*. 2006;78:5329–5347.
15. Ruthven D. *Principles of Adsorption and Adsorption Processes*. New York, NY: Wiley, 1984.
16. Landauer R. Electrical resistance of binary metallic mixtures. *J Appl Phys*. 1952;23:779–784.
17. Gritti F, Guiochon G. Measurement of hold-up volumes in reverse-phase liquid chromatography. Definition and comparison between static and dynamic methods. *J Chromatogr A*. 2007;1161:157–169.
18. Knox J, McLaren L. A new gas chromatographic method for measuring gaseous diffusion coefficients and obstructive factors. *Anal Chem*. 1964;36:1477–1482.
19. Cabooter D, Lynen F, Sandra P, Desmet G. Total pore blocking as an alternative method for the on-column determination of the external porosity of packed and monolithic reversed-phase columns. *J Chromatogr A*. 2007;1157:131–141.
20. Ludlum D, Warner R, Smith H. The diffusion of thiourea in water at 25 deg. *J Phys Chem*. 1962;66:1540–1542.
21. Dunlop P, Pepela C, Steel B. Diffusion study at 25 deg. with a shearing diffusiometer. Comparison with the Gouy and conductance methods. *J Am Chem Soc*. 1970;92:6743–6750.
22. Toulmin A, Wood J, Kenny P. Toward prediction of alkane/water partition coefficient. *J Med Chem*. 2008;51:3720–3730.
23. Poling B, Prausnitz J, O' Connel J. *The Properties of Gases and Liquids*, 5th ed. New York, NY: McGraw-Hill, 2001.
24. Wilke C, Chang P. Correlation of diffusion coefficients in dilute solutions. *AIChE J*. 1955;1:264–270.
25. Miyabe K. Evaluation of chromatographic performance of various packing materials having different structural characteristics as stationary phase for fast high performance liquid chromatography by new moment equations. *J Chromatogr A*. 2008;1183:49–64.

26. Gritti F, Guiochon G. Mass transfer kinetic mechanism in monolithic columns and application to the characterization of new research monolithic samples with different average pore sizes. *J Chromatogr A*. 2009;1216:4752–4767.
27. Gritti F, Leonardis I, Abia J, Guiochon G. Physical properties and structure of the core-shell particles used as packing materials for chromatography. A relationship between particle design and column performance. *J Chromatogr A*. In press.
28. Kaczmarski K, Guiochon G. Modeling of chromatography separation using pellicular adsorbent. *Anal Chem*. 2006;78:4648–4656.
29. Gritti F, Cavazzini A, Marchetti N, Guiochon G. Comparison between the efficiencies of columns packed with fully and partially porous $C_{18}$-bonded silica materials. *J Chromatogr A*. 2007;1157:289–303.
30. Gritti F, Leonardis I, Shock D, Stevenson P, Shalliker A, Guiochon G. Performance of columns packed with the new shell particles, Kinetex-$C_{18}$. *J Chromatogr A*. 2010;1217:1589–1603.

*Manuscript received Apr. 15, 2009, and revision received Mar. 30, 2010.*